

Collision Integrals of Discrete-Sectional Model in Simulating Powder Production

Shih-Yuan Lu

Dept. of Chemical Engineering, National Tsing-Hua University, Hsin-Chu, Taiwan 30043, ROC

Manufacture of powders through gas-phase reactions in an aerosol reactor has become increasingly important and popular since it offers a much cleaner and energy-effective route over the more traditional wet chemistry method (Ulrich, 1984; Pratsinis, 1989). The fundamentals of particle formation and growth within the reactor have thus drawn much attention from the aerosol research community (Wu et al., 1988; Landgrebe and Pratsinis, 1989, 1990a,b; Kobata et al., 1991). Many important product particle characteristics such as the geometric mean diameter and geometric standard deviation can now be studied subject to process variations by solving the discrete general aerosol dynamic equation that governs the particle-size evolution in the reactor. Solution of the discrete general aerosol dynamic equation, however, involves integration of over 10^9 simultaneous stiff ordinary differential equations to carry the simulation into useful product particle-size range, namely, the submicron range. Computing resources required to carry out this size of simulation are apparently enormous.

To circumvent the difficulty in computation, several approximation schemes have been proposed in recent years. Among them, the discrete-sectional model appeared to be the most accurate and efficient (Gelbard et al., 1980; Wu and Flagan, 1988; Landgrebe and Pratsinis, 1990b). The essence of the model is to divide the simulated particle-size range into two regimes, one discrete and the other sectional. In the discrete regime particles are treated individually, while in the sectional regime particles are lumped into sections with constant section properties. Collision rates between discrete and sectional particles are determined from the so-called collision integrals (Landgrebe and Pratsinis, 1990b). Accurate evaluation of these integrals, however, is not a trivial matter because of discontinuities embedded in the integrands. Gelbard et al. (1980) proposed a geometric sectionalization scheme that eliminates the discontinuity from the integrands and thus greatly simplifies the integral evaluation process. The scheme requires a consecutive section boundary ratio of 2. The use of consecutive section boundary ratio of 2 or larger has been adopted by many researchers in the area (Wu and Flagan, 1988; Wu et al., 1988; Kobata et al., 1991). Nevertheless, Landgrebe and Pratsinis (1990b) found that the use of geometric or coarser sectionalization schemes leads to inaccurate particle-size distributions, especially for number-based discrete-sectional

models, because of insufficient resolution in section spacing. To enable use of smaller section spacing, they developed a graphical technique that sets limits to the integrals according to combination of the discontinuity and original integration limits in a way to exclude zero integrand region, thus the discontinuities.

In this note, a rigorous analysis that removes the discontinuity from the integrand by setting the integration limits in terms of relevant size parameters is presented, offering a clearer display and more robotic programming basis of the discontinuity-free collision integrals. Notations in this note shall follow those of Landgrebe and Pratsinis (1990b).

Collision Integrals

There are eight dimensionless collision integrals defined by Landgrebe and Pratsinis (1990b) that involve discontinuous integrands. For conciseness, only the analysis for the most complicated case, production of conserved particle property Q of section- k from coagulation of smaller section- i and section- j particles, is presented; analyses for the other seven collision integrals follow the same line. The collision integral considered is given as:

$$\bar{\gamma}_{i,j,k} = \int_{b_{i-1}}^{b_i} \int_{b_{j-1}}^{b_j} \frac{\Theta(b_{k-1} < r+s \leq b_k) (r+s)^\zeta \gamma_{r,s}}{r^\zeta s^\zeta (b_i - b_{i-1})(b_j - b_{j-1})} dr ds,$$

where b_i is a particle-size parameter indicating the number of molecules in particle i , ζ a constant in defining conserved particle property, $\gamma_{r,s}$ the dimensionless coagulation coefficient between particles of sizes r and s , and Θ a discontinuous function with value 1 if its argument is satisfied, and 0 otherwise. The ranges of indexes i and j run from 1 to $k-1$, and that of k from 2 to m , with m being the number of sections used in the model.

To save space, we retain only the relevant quantity of the integrand and lump the rest to a function $f(r, s)$ as follows:

$$\bar{\gamma}_{i,j,k} = \int_{b_{i-1}}^{b_i} \int_{b_{j-1}}^{b_j} f(r, s) \Theta(b_{k-1} < r+s \leq b_k) dr ds. \quad (1)$$

Table 1. Collision Integrals of Discrete-Sectional Model for Simulating Aerosol Coagulation*

${}^1\overline{\gamma}_{i,j,k}$	$\int_{\max\{b_{j-1}, b_{k-1}-b_j\}}^{\min\{b_i, b_k-b_{j-1}\}} \int_{\max\{b_{j-1}, b_{k-1}-s\}}^{\min\{b_j, b_k-s\}} \frac{(r+s)^{\xi} \gamma_{r,s}}{r^{\xi} s^{\xi} (b_i - b_{i-1}) (b_j - b_{j-1})} dr ds$	$1 \leq i \leq k-1$ $1 \leq j \leq k-1$ $2 \leq k \leq m$	Production of section- k Q from coagulation of section- i and section- j particles
${}^2\overline{\gamma}_{i,k}$	$\int_{b_{j-1}}^{b_i} \int_{\max\{b_{k-1}, b_k-s\}}^{b_k} \frac{r^{\xi} \gamma_{r,s}}{r^{\xi} s^{\xi} (b_i - b_{i-1}) (b_k - b_{k-1})} dr ds$	$1 \leq i \leq k-1$ $2 \leq k \leq m$	Loss of section- k Q from coagulation of section- k and section- i particles
${}^3\overline{\gamma}_k$	$\int_{b_{k-1}}^{b_k} \int_{\max\{b_{k-1}, b_k-s\}}^{b_k} \frac{(r^{\xi} + s^{\xi}) \gamma_{r,s}}{r^{\xi} s^{\xi} (b_k - b_{k-1})^2} dr ds$	$1 \leq k \leq m$	Loss of section- k Q from coagulation of section- k and section- k particles
${}^5\overline{\gamma}_{i,k}$	$\int_{b_{j-1}}^{\min\{b_i, b_k-b_{j-1}\}} \int_{b_{k-1}}^{b_k-s} \frac{((r+s)^{\xi} - r^{\xi}) \gamma_{r,s}}{r^{\xi} s^{\xi} (b_i - b_{i-1}) (b_k - b_{k-1})} dr ds$	$1 \leq i \leq k-1$ $2 \leq k \leq m$	Production of section- k Q from coagulation of section- k and section- i particles
${}^6\overline{\gamma}_k$	$\int_{b_{k-1}}^{b_k-b_{k-1}} \int_{b_{k-1}}^{b_k-s} \frac{((r+s)^{\xi} - (r^{\xi} + s^{\xi})) \gamma_{r,s}}{r^{\xi} s^{\xi} (b_k - b_{k-1})^2} dr ds$	$1 \leq k \leq m$	Production of section- k Q from coagulation of section- k and section- k particles
${}^1\overline{\gamma}_{i,j,k}^D$	$\int_{\max\{b_{j-1}, b_{k-1}-i\}}^{\min\{b_j, b_k-i\}} \frac{(i+r)^{\xi} \gamma_{i,r}}{i^{\xi} r^{\xi} (b_j - b_{j-1})} dr$	$1 \leq i \leq i_{\max}$ $1 \leq j \leq k-1$ $2 \leq k \leq m$	Production of section- k Q from coagulation of an i -sized particle and section- j particles
${}^2\overline{\gamma}_{i,k}^D$	$\int_{\max\{b_{k-1}, b_k-i\}}^{b_k} \frac{r^{\xi} \gamma_{i,r}}{i^{\xi} r^{\xi} (b_k - b_{k-1})} dr$	$1 \leq i \leq i_{\max}$ $1 \leq k \leq m$	Loss of section- k Q from coagulation of section- k particles and an i -sized particle
${}^5\overline{\gamma}_{i,k}^D$	$\int_{b_{k-1}}^{b_k-i} \frac{((i+r)^{\xi} - r^{\xi}) \gamma_{i,r}}{i^{\xi} r^{\xi} (b_k - b_{k-1})} dr$	$1 \leq i \leq i_{\max}$ $1 \leq k \leq m$	Production of section- k Q from coagulation of an i -sized particle and section- k particles

* i_{\max} is the number of discrete sizes used in the model and Q is a conserved particle property (such as particle number, particle volume, and squared particle volume) in the sectional regime. Also note that the integral value is 0 when the upper limit is less than the lower limit in the outer integration.

We consider first the outer integration. The outer integration dummy variable s falls within $[b_{j-1}, b_i]$. Also from the restriction of the discontinuous function Θ , s must satisfy the following two inequalities to ensure nonzero integrands:

$$\begin{aligned} s &\leq b_k - b_{j-1}, \\ s &> b_{k-1} - b_j. \end{aligned}$$

Choosing the most restrictive limits ensures nonzero integrands within the integration interval. With this, the upper and lower limits of the outer integration can be specified as $\min\{b_i, b_k - b_{j-1}\}$ and $\max\{b_{j-1}, b_{k-1} - b_j\}$, respectively. It is implied that the integral value is 0 if the upper limit is less than the lower limit.

For a given s , the inner integration limits can be set following the same line of analysis. The inner integration dummy variable r , which runs from b_{j-1} to b_j , is restricted by the following two constraints,

$$\begin{aligned} r &\leq b_k - s, \\ r &> b_{k-1} - s. \end{aligned}$$

The inner upper and lower integration limits thus become $\min\{b_j, b_k - s\}$ and $\max\{b_{j-1}, b_{k-1} - s\}$, respectively. The collision integral of Eq. 1 then takes the following form,

$${}^1\overline{\gamma}_{i,j,k} = \begin{cases} 0, & \text{if } \min\{b_i, b_k - b_{j-1}\} < \max\{b_{j-1}, b_{k-1} - b_j\}, \\ \int_{\max\{b_{j-1}, b_{k-1}-b_j\}}^{\min\{b_i, b_k-b_{j-1}\}} \int_{\max\{b_{j-1}, b_{k-1}-s\}}^{\min\{b_j, b_k-s\}} f(r, s) dr ds. \end{cases}$$

Analyses for the other seven collision integrals follow the same line. The results are tabulated in Table 1.

Numerical Integration

The collision integrals in Table 1 have now possessed no discontinuities in the integrands. Standard numerical integration schemes such as Gauss-Legendre quadrature (see, for example, Press et al., 1992) can be applied to evaluate these integrals. There is, however, one more fine point to be mentioned. When the outer integration dummy variable s steps from the lower limit to upper limit, the length of the inner integration interval may experience discontinuous slope changes characterized by two discontinuous points at most. The slope discontinuity of the inner integration interval length, to an appreciable extent, damages the accuracy and convergence of the applied numerical integration scheme. It is strongly recommended that the outer integration interval be divided into two or three portions if there are one or two slope discontinuous points. There are two potential discontinuous points for ${}^1\overline{\gamma}_{i,j,k}$, $s = b_k - b_j$ and $s = b_{k-1} - b_{j-1}$. These two points qualify to be discontinuous points if they fall between the lower and upper limits, $\max\{b_{j-1}, b_{k-1} - b_j\}$ and $\min\{b_i, b_k - b_{j-1}\}$. ${}^1\overline{\gamma}_{i,j,k}$, ${}^2\overline{\gamma}_{i,k}$, and ${}^3\overline{\gamma}_k$ are the three collision integrals that may encounter the

Table 2. Potential Discontinuous Points in Outer Integration Interval of ${}^1\overline{\gamma}_{i,j,k}$, ${}^2\overline{\gamma}_{i,k}$, and ${}^3\overline{\gamma}_k$

${}^1\overline{\gamma}_{i,j,k}$	$b_k - b_j$ $b_{k-1} - b_{j-1}$
${}^2\overline{\gamma}_{i,k}$	$b_k - b_{k-1}$
${}^3\overline{\gamma}_k$	$b_k - b_{k-1}$

slope discontinuity. Table 2 lists potential discontinuous points for the three collision integrals, and Figure 1 shows a case of discontinuous slope changes.

Collision Summations

Collision integrals were originally derived based on a continuous representation of the particle-size variable. Since a particle can contain only integer number of molecules, collision rates based on a discrete representation of the particle-size variable offer a more accurate account of the coagulation process (Gelbard et al., 1980). The resulting collision rate constants are summations with summands identical to the integrands of corresponding collision integrals. Table 3 summarizes the discontinuity-free collision summations.

It is to be noted that, although collision summations are a better choice over the collision integrals, the evaluation of collision summations is computationally much more expensive, especially for summations with large-size intervals. To see this, consider a typical discrete-sectional model of 20 discrete size entities and 50 sections with a consecutive section boundary ratio (referred to as the section spacing factor in Landgrebe and Pratsinis, 1990) of 1.5. Take the evaluation of $\bar{\gamma}_{20,20,21}$, for example, a Gauss-Legendre 20-point quadrature is sufficient to calculate the collision integral accurate to the 14th significant figure, needing only 441 integrand evaluations. As for the collision summation approach, one needs, for the present model, 61,421,986 integrand evaluations. Assuming each integrand evaluation requires N floating operations, it would

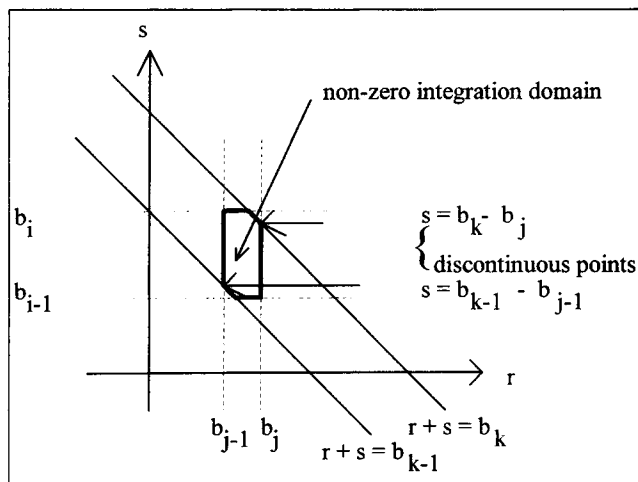


Figure 1. Discontinuous slope changes in inner integration interval for a case of $\bar{\gamma}_{i,j,k}$.

take a computer capable of executing 26 million floating points operations per second (MFLOPS) such as a DEC alpha 3000/400 AXP workstation about $2.34(N+1)$ s ($2.34N$ s for integrand evaluations and 2.34 s for the summation) to calculate just one component of $\bar{\gamma}_{i,j,k}$.

Fortunately, with large-size intervals, summations approach integrals as in Figure 2. The relative error of the collision rate constants calculated by the integral approach vs. the sum-

Table 3. Collision Summations of Discrete-Sectional Model for Simulating Aerosol Coagulation*

$\bar{\gamma}_{i,j,k}^1$	$\sum_{l=\max\{b_{j-1}, b_k-b_{j-1}+1\}}^{\min\{b_i, b_k-b_{j-1}\}} \sum_{n=\max\{b_{j-1}, b_{k-1}-l+1\}}^{\min\{b_i, b_k-l\}} \frac{(n+l)^{\frac{1}{2}} \gamma_{n,l}}{n^{\frac{1}{2}} l^{\frac{1}{2}} (b_i - b_{i-1}) (b_j - b_{j-1})}$	$1 \leq i \leq k-1$ $1 \leq j \leq k-1$ $2 \leq k \leq m$	Production of section- k Q from coagulation of section- i and section- j particles
$\bar{\gamma}_{i,k}^2$	$\sum_{l=b_{j-1}+1}^{b_j} \sum_{n=\max\{b_{k-1}, b_k-l+1\}}^{b_k} \frac{n^{\frac{1}{2}} \gamma_{n,l}}{n^{\frac{1}{2}} l^{\frac{1}{2}} (b_i - b_{i-1}) (b_k - b_{k-1})}$	$1 \leq i \leq k-1$ $2 \leq k \leq m$	Loss of section- k Q from coagulation of section- k and section- i particles
$\bar{\gamma}_k^3$	$\sum_{l=b_{k-1}+1}^{b_k} \sum_{n=\max\{b_{k-1}, b_k-l+1\}}^{b_k} \frac{(n^{\frac{1}{2}} + l^{\frac{1}{2}}) \gamma_{n,l}}{n^{\frac{1}{2}} l^{\frac{1}{2}} (b_k - b_{k-1})^2}$	$1 \leq k \leq m$	Loss of section- k Q from coagulation of section- k and section- k particles
$\bar{\gamma}_{i,k}^4$	$\sum_{l=b_{j-1}+1}^{b_j} \sum_{n=b_{k-1}+1}^{b_k} \frac{n^{\frac{1}{2}} \gamma_{n,l}}{n^{\frac{1}{2}} l^{\frac{1}{2}} (b_i - b_{i-1}) (b_k - b_{k-1})}$	$k+1 \leq i \leq m$ $1 \leq k \leq m-1$	Loss of section- k Q from coagulation of section- k and larger particles
$\bar{\gamma}_{i,k}^5$	$\sum_{l=b_{j-1}+1}^{\min\{b_i, b_k-b_{k-1}\}} \sum_{n=b_{k-1}+1}^{b_k-l} \frac{((n+l)^{\frac{1}{2}} - n^{\frac{1}{2}}) \gamma_{n,l}}{n^{\frac{1}{2}} l^{\frac{1}{2}} (b_i - b_{i-1}) (b_k - b_{k-1})}$	$1 \leq i \leq k-1$ $2 \leq k \leq m$	Production of section- k Q from coagulation of section- k and section- i particles
$\bar{\gamma}_k^6$	$\sum_{l=b_{k-1}+1}^{b_k-b_{k-1}} \sum_{n=b_{k-1}+1}^{b_k-l} \frac{((n+l)^{\frac{1}{2}} - (n^{\frac{1}{2}} + l^{\frac{1}{2}})) \gamma_{n,l}}{n^{\frac{1}{2}} l^{\frac{1}{2}} (b_k - b_{k-1})^2}$	$1 \leq k \leq m$	Production of section- k Q from coagulation of section- k and section- k particles
$\bar{\gamma}_{i,j,k}^{1D}$	$\sum_{n=\max\{b_{j-1}, b_k-b_{j-1}-i+1\}}^{\min\{b_i, b_k-i\}} \frac{(i+n)^{\frac{1}{2}} \gamma_{i,n}}{i^{\frac{1}{2}} n^{\frac{1}{2}} (b_j - b_{j-1})}$	$1 \leq i \leq i_{\max}$ $1 \leq j \leq k-1$ $2 \leq k \leq m$	Production of section- k Q from coagulation of an i -sized particle and section- j particles
$\bar{\gamma}_{i,k}^{2D}$	$\sum_{n=\max\{b_k-b_{k-1}-i+1\}}^{b_k} \frac{n^{\frac{1}{2}} \gamma_{i,n}}{i^{\frac{1}{2}} n^{\frac{1}{2}} (b_k - b_{k-1})}$	$1 \leq i \leq i_{\max}$ $1 \leq k \leq m$	Loss of section- k Q from coagulation of section- k particles and an i -sized particle
$\bar{\gamma}_{i,k}^{4D}$	$\sum_{n=b_{k-1}+1}^{b_k} \frac{i^{\frac{1}{2}} \gamma_{i,n}}{i^{\frac{1}{2}} n^{\frac{1}{2}} (b_k - b_{k-1})}$	$1 \leq i \leq i_{\max}$ $1 \leq k \leq m$	Loss of q_i from coagulation of i -sized and section- k particles
$\bar{\gamma}_{i,k}^{5D}$	$\sum_{n=b_{k-1}+1}^{b_k-i} \frac{((i+n)^{\frac{1}{2}} - n^{\frac{1}{2}}) \gamma_{i,n}}{i^{\frac{1}{2}} n^{\frac{1}{2}} (b_k - b_{k-1})}$	$1 \leq i \leq i_{\max}$ $1 \leq k \leq m$	Production of section- k Q from coagulation of an i -sized particle and section- k particles

* q_i is a conserved particle property (such as particle number, particle volume, and squared particle volume) of i -sized particles in the discrete regime.

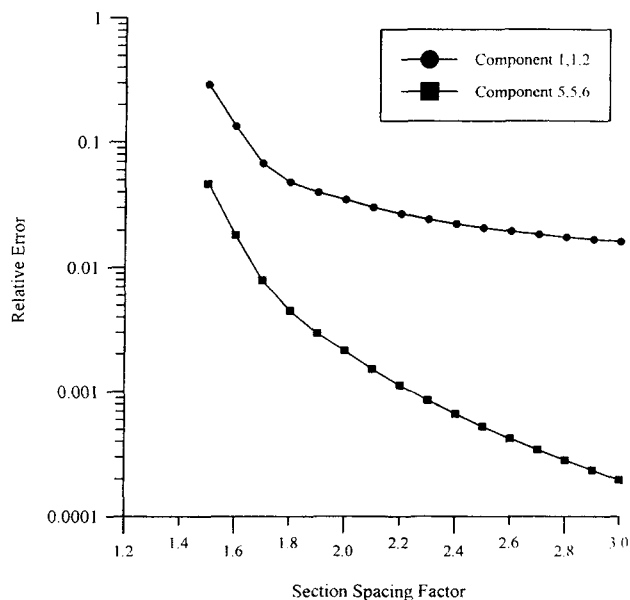


Figure 2. Relative error of $\bar{\gamma}_{1,1,2}$ and $\bar{\gamma}_{5,5,6}$ vs. section spacing factor.

mation approach is plotted against the section spacing factor. Size intervals increase with increasing section spacing factor resulting in decrease in the relative error as expected. The relative error of $\bar{\gamma}_{i,j,k}$ of a smaller size interval ($\bar{\gamma}_{1,1,2}$) is much larger than the relative error of $\bar{\gamma}_{i,j,k}$ of a larger-size interval ($\bar{\gamma}_{5,5,6}$) for a fixed section spacing factor. It is thus recommended to use collision summations for collision rate constants with small-size intervals and collision integrals for collision rate constants with large-size intervals.

Acknowledgment

This research was supported by the National Science Council of the Republic of China under grant number NSC 83-0402-E-007-021.

Notation

b_i = particle-size parameter indicating number of molecules in particle i

f = function of r and s

i_{\max} = number of discrete sizes used in the discrete-sectional model

m = number of sections used in the discrete-sectional model

q = conserved particle property in the discrete regime

Q = conserved particle property in the sectional regime

r, s = integration dummy variables

Greek letters

$\gamma_{i,j}$ = dimensionless coagulation coefficient between particles for sizes i and j

$\bar{\gamma}$ = dimensionless collision integral for coagulation between particles in two sections

$\bar{\gamma}^D$ = dimensionless collision integral for coagulation between a discrete particle and particles in a section

ξ = particle property constant

Θ = discontinuous function

Literature Cited

- Gelbard, F., Y. Tambour, and J. H. Seinfeld, "Sectional Representations for Simulating Aerosol Dynamics," *J. Colloid Interf. Sci.*, **76**, 541 (1980).
- Kobata, A., K. Kusakabe, and S. Morooka, "Growth and Transformation of TiO_2 Crystallites in Aerosol Reactor," *AIChE J.*, **37**, 347 (1991).
- Landgrebe, J. D., and S. E. Pratsinis, "Gas-Phase Manufacture of Particulates: Interplay of Chemical Reaction and Aerosol Coagulation in the Free-Molecular Regime," *Ind. Eng. Chem. Res.*, **28**, 1474 (1989).
- Landgrebe, J. D., and S. E. Pratsinis, "Nomographs for Vapor Synthesis of Ceramic Powders," *Chem. Eng. Sci.*, **45**, 2931 (1990a).
- Landgrebe, J. D., and S. E. Pratsinis, "A Discrete-Sectional Model for Particulate Production by Gas-Phase Chemical Reaction and Aerosol Coagulation in the Free-Molecular Regime," *J. Colloid Interf. Sci.*, **139**, 63 (1990b).
- Pratsinis, S. E., "Material Synthesis in Aerosol Reactors," *Chem. Eng. Prog.*, **85**, 62 (1989).
- Press, W. H., S. A. Teukolsky, W. T. Vetterling, and B. P. Flannery, *Numerical Recipes in FORTRAN*, Cambridge University Press, New York, Section 4.5 (1992).
- Ulrich, G. D., "Flame Synthesis of Fine Particles," *Chem. & Eng. N.*, **62**, 22 (1984).
- Wu, J. J., and R. C. Flagan, "A Discrete-Sectional Solution to the Aerosol Dynamic Equation," *J. Colloid Interf. Sci.*, **123**, 339 (1988).
- Wu, J. J., H. V. Nguyen, R. C. Flagan, K. Okuyama, and Y. Kousaka, "Evaluation and Control of Particle Properties in Aerosol Reactors," *AIChE J.*, **34**, 1249 (1988).

Manuscript received Aug. 23, 1993, and revision received Oct. 18, 1993.